THE FINITE ELEMENT EVALUATION OF SUPPORT BRACKET USING THE APPLICATION OF TOPOLOGICAL OPTIMIZATION

DOI : 10.36909/jer.ICIPPSD.15505

Letsatsi M.T. *, Agarwal A. **, Pitso I.**

*Department of Industrial Design & Technology, FET, University of Botswana, Gaborone, Botswana.

** Department of Mechanical Engineering, FET, University of Botswana, Gaborone, Botswana

* Corresponding Author: letsatsim@ub.ac.bw

ABSTRACT

The demand for customized products has increased to suite various needs which could be easily developed using 3D printing technology. Most of the products require optimization for weight minimization which could be done using topological optimization tool. Topology optimization offers conceptual design for lighter and stiffer structures and helps to reach to efficient and aesthetic designs in lesser time. Topological optimization has shown its effectiveness is in improving design of structures with the help of high configuration and fast computing processors. With the use of FEA, the topologically optimized design can be tested which enables to determine design feasibility for different loads and boundary conditions. The current research investigates the application of topological optimization tool in weight minimization of support bracket. The generic design of supporting bracket is developed in Creo design software and structural analysis is conducted using techniques of Finite Element Method. The topological optimization tool enabled to reduce nearly 32% mass without much increase in deformation and stresses. The increase in deformation was found to be 5.6% and is profound in the regions of cylindrical support structure.

Key words: Support bracket; design; additive manufacturing; topological optimization; finite element analysis.

INTRODUCTION

The additive manufacturing process involves layer by layer addition of material whereas subtractive manufacturing refers to removal of material by various machining processes. These machining process may include finishing, knurling, tapering, milling etc. The layers of materials added in additive manufacturing ranges from .06mm to .04mm thick and may take

time. The quality of produced object depends upon various factors. Out of which the 3D printing method, layer thickness and structure are most significant. Some of the widely used 3D printing technologies are Digital Light Processing (DLP) and Fused Deposition Modelling (FDM) (Anon n.d.). Al-ahmari, Mian, and Ameen (2021) have conducted research to identify various sources of errors that contribute to the poor accuracy of Fused deposition modeling (FDM) fabricated parts. A standard part comprised of a variety of contours, characteristics, and geometries, was used for the evaluation of the FDM process & provided the valuable information.

One of the important advantages of AM is its capability to produce complex geometries without any need of dies. The desired dimensions of component can be attained without any need for machining (Ullen, Hasak, and Dirikolu, 2020).

Another important advantage of AM has shorter lead time and less wastage of material as compared to conventional subtractive manufacturing (Ngo et al., 2018). Hu and Zhao (2020) studied the alternative path scheme on structural nonlinear dynamic history analysis and 3-D .

Finite element modelling was done for steel composite frame structure with considering the contribution of the composite behavior. The most commonly used material for 3D printing is maraging steel (Casalino et al., 2015), austenitic stainless steel (Carlton et al., 2016), stainless steels (Murr et al. 2012) and tool steels (Mazumder et al., 1997). Sen, Yilmaz, and Yildiz (2020) have performed the finite element analysis to determine the degree of spring back of six different sheet metal thickness along with other properties taking into consideration the mechanical properties as per ASTM standards.

Zhong et al. (2017) has worked on 3D printing of Portland cement free concrete using nano-graphene oxide. The strength of concrete was found to be 30MPa and electrical conductivity was high. The finer resolution of concrete was printed using polyvinyl alcohol (PVA) composite. Zhu et al. (2017) has 3D printed cementitious mortar using SAC which is Sulpho-Aluminate Cement and Ordinary Portland cement (OPC). The findings have shown that Sulpho-aluminate cement (SAC) is better than Ordinary Portland cement (OPC) due to shorter setting time and higher early strength. For 3D printing, the faster setting time is desirable as it allows "bottom layer to develop good strength in order to support top layers". Li et al. (2020) has found that nozzle shape, material, speed, and feed are important printing parameters which determine the quality of printed product. Zareiyan and Khoshnevis (2017) has investigated the factors affecting bond strength between layers of 3D printed concrete. The results have shown that aggregate size and layer thickness have significant effect on quality and strength of 3D

printed concrete. Kazemian et al. (2017) has worked on shape stability of 3D printed paste and found that use of silica fume along with nano clay can significantly enhance stability. Xia and Sanjayan (2016) has investigated 3D printing using the geopolymer material. The material comprises of alkali activator, furnace slag and liquid binder consists of pyrrolidone. The 3D printed cubes have lower strength and subsequently treated with alkali solution which augmented strength by 15.9MPa.

In the current research, the mass of support bracket (used in hydraulic cylinder) is reduced using techniques of topological optimization. The static structural analysis is conducted on generic and optimized design (topological optimized) using techniques of finite element method. The software used for static structural analysis is ANSYS and comparison is made for generic design, topologically optimized design on the parameters of deformation and equivalent stress generated.

METHODOLOGY

The FEA analysis is conducted on generic design of support bracket using ANSYS FEA software which involves 3 stages i.e., preprocessing, solution and postprocessing. The developed CAD model is analyzed using ANSYS FEA software (Agarwal and Pitso, 2020). Using Creo design software, the first generic design of support braket is developed using extrude, round tool as shown in figure 1.

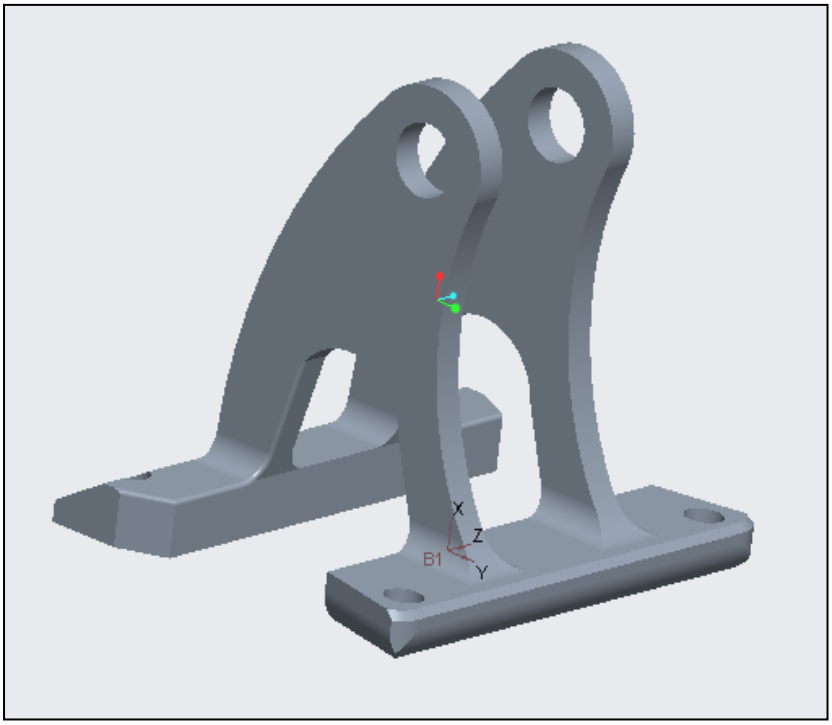

Figure 1 CAD model of generic design of support bracket

The FEA analysis procedure involves importing CAD model in figure 2 shows meshing, applying loads and boundary conditions. The discretized model of support bracket is shown in figure 3 while load and boundary conditions are shown in figure 4.

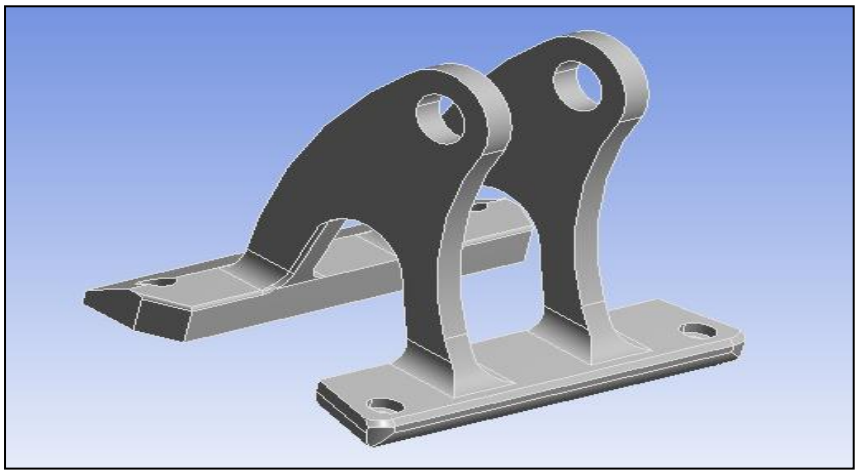

Figure 2 Imported CAD model

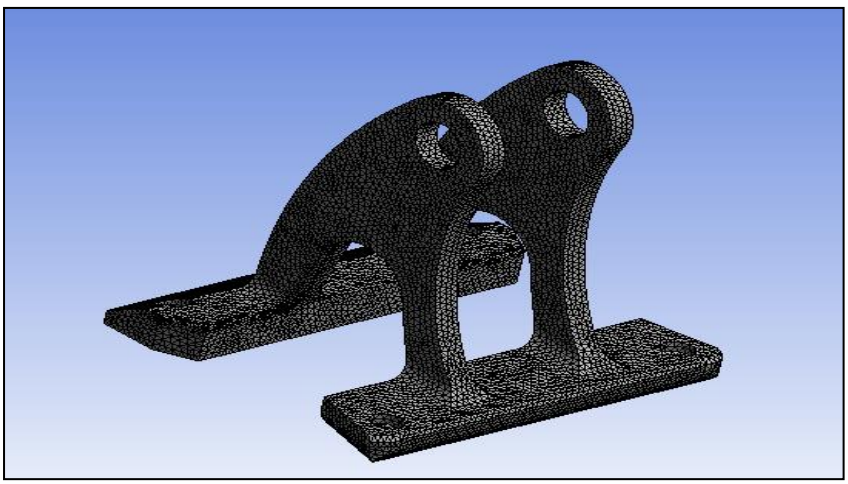

Figure 3 Meshed model of support bracket

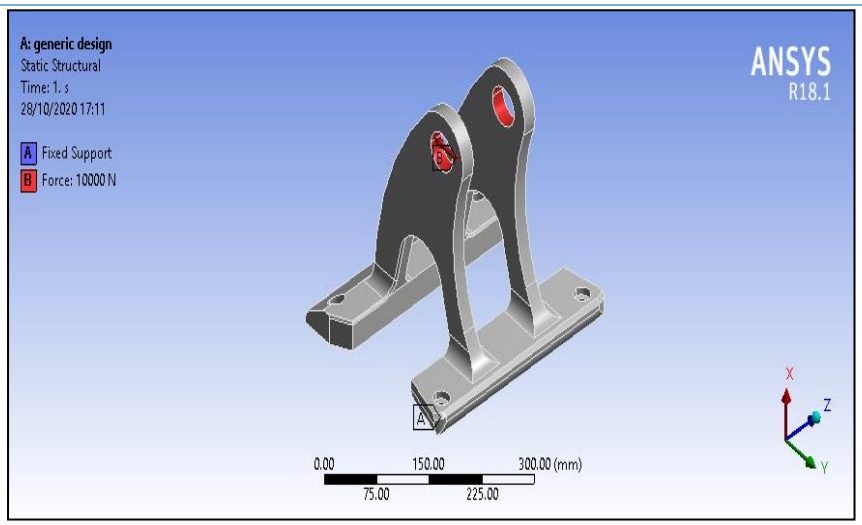

Figure 4 Loads and boundary condition.

Due to complexity of structure tetrahedral element type is used for meshing. The element type is tetrahedral, (Agarwal and Letsatsi, 2020) and number of elements generated is 118695 and number of nodes generated is 182358. The model is subjected to static loading conditions with fixed support on bottom face and 10000N load on cylindrical surface. After applying loads and boundary condition, the simulation is run using "sparse matrix solver which involves matrix formulation, matrix multiplications and inversions. The material used for analysis is ABS plastics. The results are calculated at nodes and interpolated for entire element edge length (Kentli, 2020). In the current research density based topological optimization technique is used. The general form of topological optimization problem is given by (Dems 1991; Querin et al., 2017)

Minimize $\rho F = F(u(\rho), \rho) = \int\Omega f(u(\rho), \rho)\, dV$; Subject to $G_0(\rho) = \int_\Omega \rho dV - V_0$

$$G_j(u(\rho), \rho) \leq 0 \text{ with } j = 1, \ldots, m \qquad (1)$$

The problem statement includes the following:

• An objective function F (u($\boldsymbol{\rho}$), $\boldsymbol{\rho}$)

• material distribution. $\boldsymbol{\rho}$(u)

• The design 0space u($\boldsymbol{\rho}$)

Such optimization is "most commonly done using the finite element method since these equations do not have a known analytical solution (Casalino et al., 2015).

RESULT AND DISCUSSION

After performing preprocessing operations and running the simulation, the equivalent stress, deformation plots are obtained for generic design and topologically optimized design. The deformation plot is obtained for generic design as shown in figure 5.

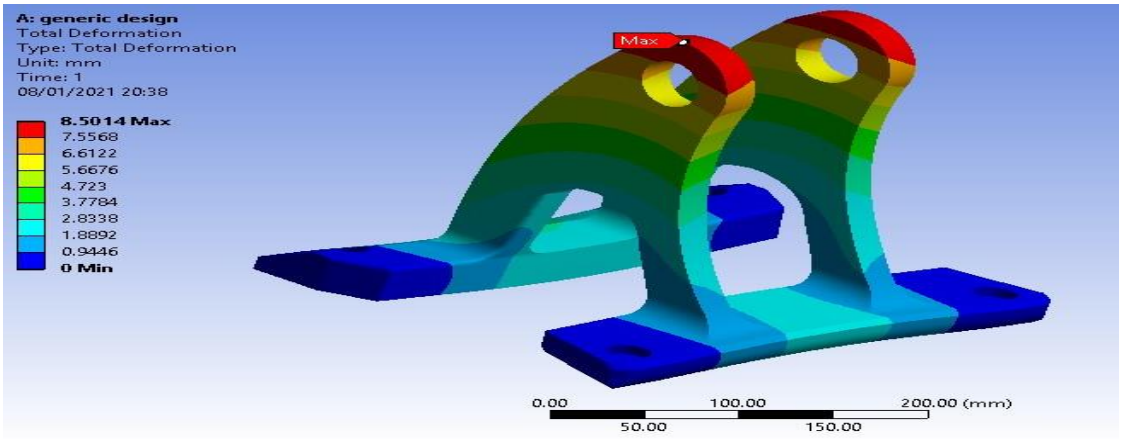

Figure 5 Deformation plot

The deformation is maximum on cylindrical region (load application) and reduces towards base. The maximum deformation obtained in generic design is 8.5mm. The equivalent stress plot is obtained as shown in figure 6. The plot shows higher equivalent stress on regions between vertical support features. The stresses on these locations are nearly 53MPa.

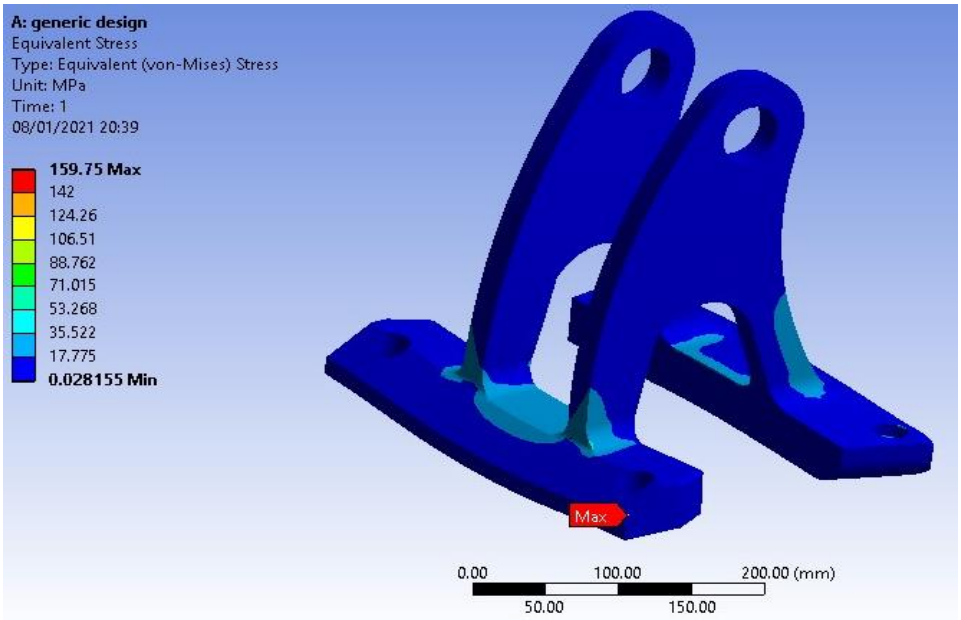

Figure 6 Equivalent stress plot

The topologically optimized support bracket is shown in figure 7. The maximum mass removal location is observed at the vicinity of top cylindrical region and regions just below it. The deformation plot is obtained for topologically optimized design as shown in figure 8.

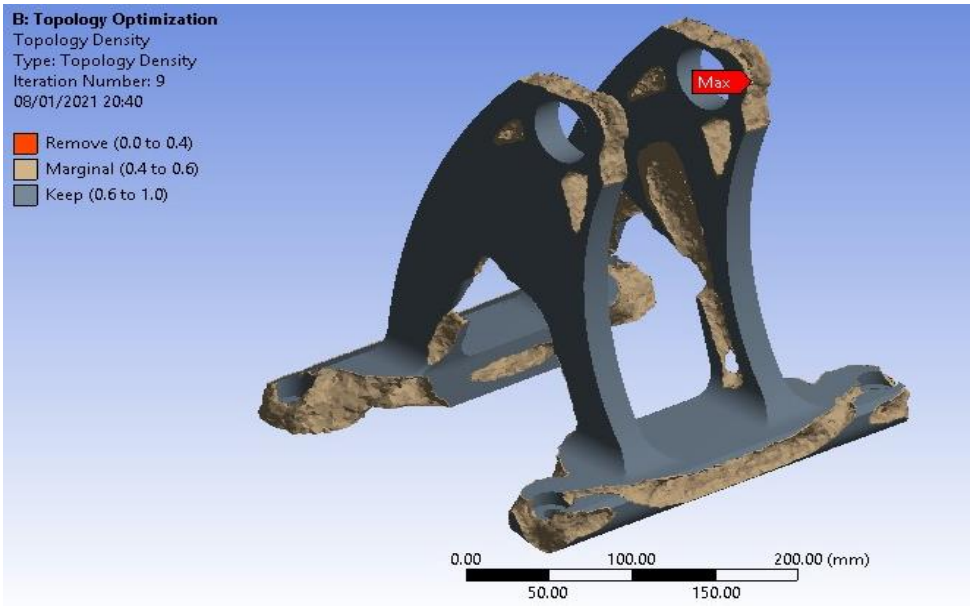

Figure 7 Topological density plot

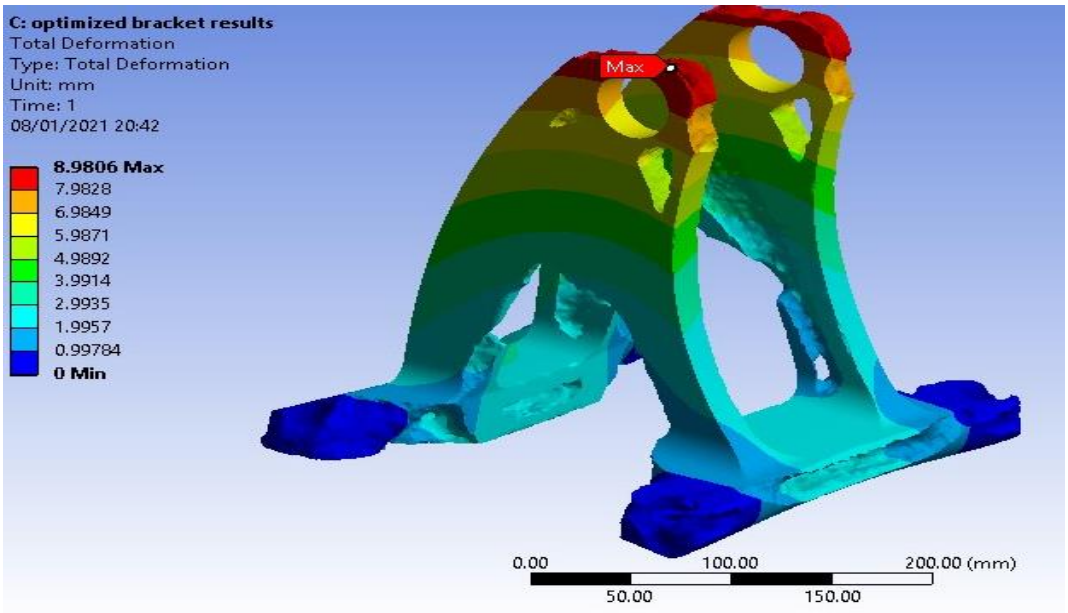

Figure 8 Deformation plot

The deformation plot shows similar pattern as in generic design i.e., the deformation is maximum on cylindrical region (load application) and reduces towards base.

The maximum deformation obtained in topologically optimized design is 8.9mm which is .4mm higher than generic design.

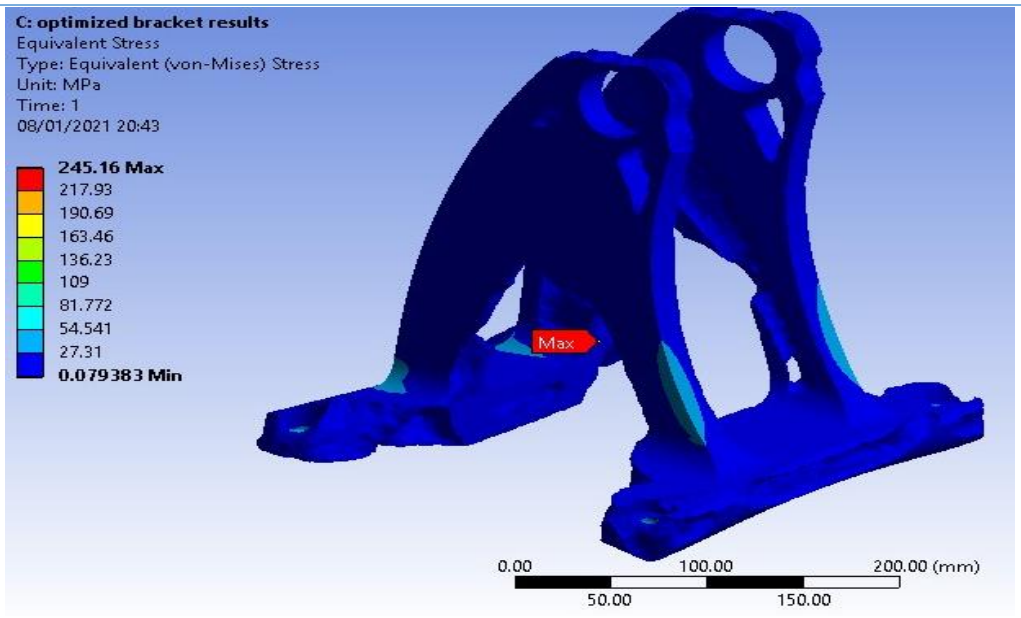

Figure 9 Equivalent stress plot

For topologically optimized design, the location of maximum equivalent stress changed as compared from generic design as shown in figure 9. The location of maximum equivalent stress is observed at one end of support feature with magnitude of 246 MPa nearly. Results of optimization performed are shown in Table 1.

Table 1 Results of optimization

Cases	**Generic Design**	**Topological Optimized Design**
Equivalent Stress (MPa)	159.75	246
Deformation(mm)	8.52	8.97
Mass (Kg)	3.16	2.17

The mass comparison plot is shown in figure 10. The plot shows 31.32% lower mass for topologically optimized design as compared to generic design.

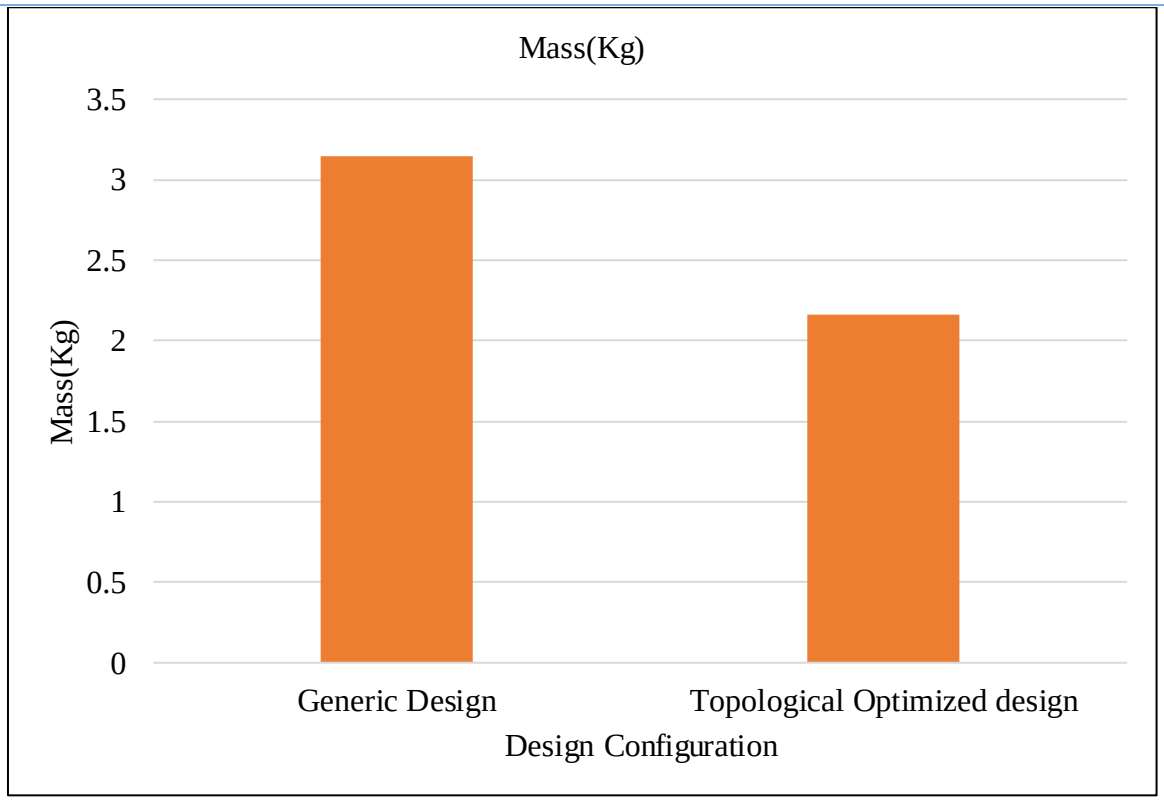

Figure 10 Mass comparison plot

The comparison plot of equivalent stress (figure 11) shows topologically optimized support bracket has higher equivalent stress as compared to generic design.

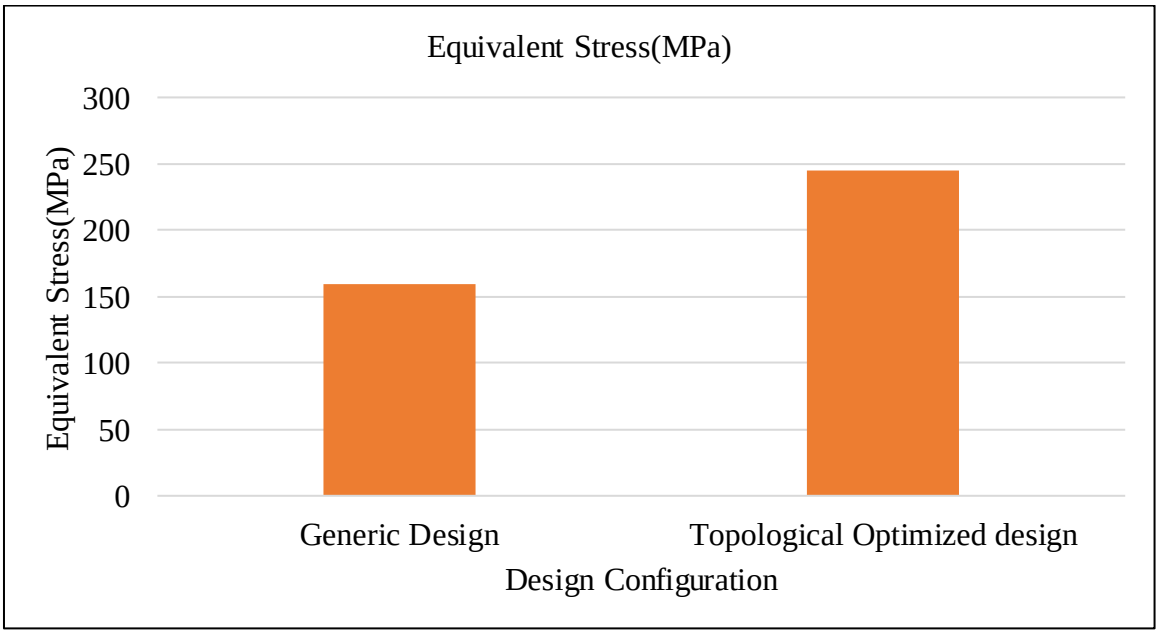

Figure 11 Equivalent stress plot

Similarly, the deformation plot as shown in figure 12, also shows higher deformation for topological optimized bracket. The deformation obtained in topological optimized design is 8.97mm and equivalent stress generated in topologically optimized design is 246 MPa.

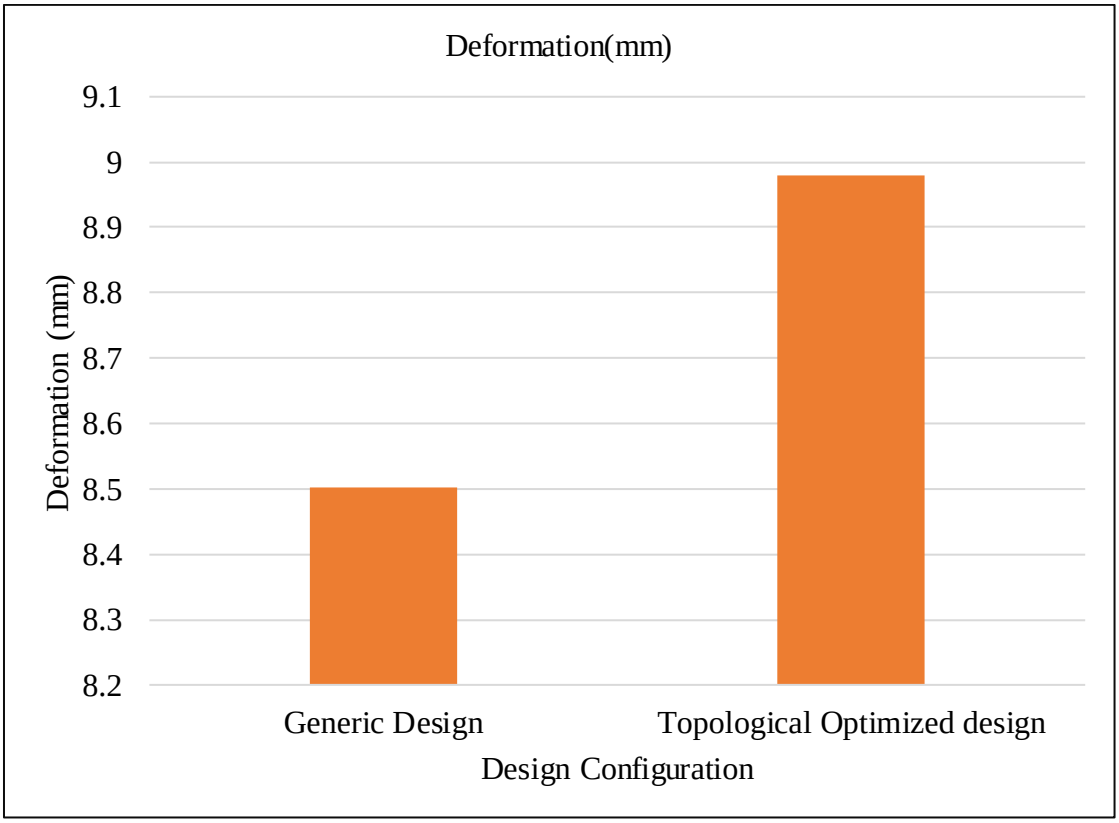

Figure 12 Deformation comparison plot

CONCLUSION

The topological optimization enabled to achieve significant mass reduction of support bracket and identified zone of mass reduction. The optimized design of support bracket has higher deformation and stress. The location of maximum stress also changed in topologically optimized design of support bracket. Different region of support bracket has different mass removal rate. The bottom regions of support feature have higher mass removal rate and side regions has marginal removal rate.

1. The mass reduction obtained using topological optimization is nearly 32 percent.

2. The equivalent stress generated for topologically optimized bracket is 53.4% higher than generic design bracket.

3. The deformation obtained for topologically optimized bracket is 5.6% higher than generic design.

The topological optimization tool can be used in other components used in automobiles and aerospace. The FEA has proved to be viable tool and topologically optimized component can be used in tested using FEA.

REFERENCES

Agarwal, A. and M. T. Letsatsi. 2021. Heat Transfer Characteristics of Flame Jet Impingement with Methane Air Reaction Environment. Materials Today: Proceedings 39(1);789-795.

Agarwal, A. and I. Pitso. 2020. Modelling & Numerical Exploration of Pulsejet Engine Using Eddy Dissipation Combustion Model. Materials Today: Proceedings 27(2):1341–49.

Al-ahmari, Abdulrahman, Syed Hammad Mian, and Wadea Ameen. 2021. Performance Assessment of Fused Deposition Modeling Process. 9(March):200–213.

Anon. n.d. Types of 3D Printers or 3D Printing Technologies Overview. 3 D Pronting from Scratch. Retrieved November 11, 2019 (http://3dprintingfromscratch.com/common/types-of-3d-printers-or-3d-printing-technologies-overview/).

Carlton, Holly D., Abdel Haboub, Gilbert F. Gallegos, Dilworth Y. Parkinson, and Alastair A. MacDowell. 2016. Damage Evolution and Failure Mechanisms in Additively Manufactured Stainless Steel. Materials Science and Engineering: A 651:406–14.

Casalino, G., S. L. Campanelli, N. Contuzzi, and A. D. Ludovico. 2015. Experimental Investigation and Statistical Optimisation of the Selective Laser Melting Process of a Maraging Steel. Optics & Laser Technology 65:151–58.

Dems, K. 1991. First- and Second-Order Shape Sensitivity Analysis of Structures. Structural Optimization 3(2):79–88.

Hu, Yi and Junhai Zhao. 2020. Layout of Cross Braces on Progressive Collapse Analysis of a 3D 12-Story Steel Composite Frame Structures. Journal of Engineering Research (Kuwait) 8(2):45–58.

Kazemian, Ali, Xiao Yuan, Evan Cochran, and Behrokh Khoshnevis. 2017. Cementitious Materials for Construction-Scale 3D Printing: Laboratory Testing of Fresh Printing Mixture. Construction and Building Materials 145:639–47.

Kentli, Aykut. 2020. Topology Optimization Applications on Engineering Structures." in Truss and Frames, edited by A. Kentli. Rijeka: IntechOpen.

Li, Zhanzhao, Maryam Hojati, Zhengyu Wu, Jonathon Piasente, Negar Ashrafi, José P. Duarte, Shadi Nazarian, Sven G. Bilén, Ali M. Memari, and Aleksandra Radlińska. 2020.

Fresh and Hardened Properties of Extrusion-Based 3D-Printed Cementitious Materials: A Review. Sustainability (Switzerland) 12(14):1–33.

Mazumder, J., J. Choi, K. Nagarathnam, J. Koch, and D. Hetzner. 1997. The Direct Metal Deposition of H13 Tool Steel for 3-D Components. JOM 49(5):55–60.

Murr, Lawrence E., Edwin Martinez, Jennifer Hernandez, Shane Collins, Krista N. Amato, Sara M. Gaytan, and Patrick W. Shindo. 2012. Microstructures and Properties of 17-4 PH Stainless Steel Fabricated by Selective Laser Melting. Journal of Materials Research and Technology 1(3):167–77.

Ngo, Tuan D., Alireza Kashani, Gabriele Imbalzano, Kate T. Q. Nguyen, and David Hui. 2018. Additive Manufacturing (3D Printing): A Review of Materials, Methods, Applications and Challenges. Composites Part B: Engineering 143:172–96.

Querin, Osvaldo M., Mariano Victoria, Cristina Alonso, Rubén Ansola, and Pascual Martí. 2017. Chapter 2 - Growth Method for the Size, Topology, and Geometry Optimization of Truss Structures**Additional Author for This Chapter Is Dr. Pedro Jesús Martínez Castejón. Pp. 15–26 in Topology Design Methods for Structural Optimization, edited by O. M. Querin, M. Victoria, C. Alonso, R. Ansola, and P. Martí. Oxford: Academic Press.

Sen, Hakan, Safak Yilmaz, and Rasid Ahmed Yildiz. 2020. Springback Behavior of DP600 Steel: An Implicit Finite Element Simulation." Journal of Engineering Research (Kuwait) 8(2):252–64.

Ullen, N. Beköz, S. M. A. Hasak, and M. H. Dirikolu. 2020. Factors Influencing the Machinability during Turning Sinter-Hardened Cu-Ni-Mo Based Steel: Dependency on Cutting Speed, Feed Rate, and Cutting Depth." Journal of Engineering Research 8(4):236–57.

Xia, Ming and Jay Sanjayan. 2016. Method of Formulating Geopolymer for 3D Printing for Construction Applications. Materials & Design 110:382–90.

Zareiyan, Babak and Behrokh Khoshnevis. 2017. Interlayer Adhesion and Strength of Structures in Contour Crafting - Effects of Aggregate Size, Extrusion Rate, and Layer Thickness. Automation in Construction 81:112–21.

Zhong, Jing, Guo-Xiang Zhou, Pei-Gang He, Zhi-Hua Yang, and De-Chang Jia. 2017. 3D Printing Strong and Conductive Geo-Polymer Nanocomposite Structures Modified by Graphene Oxide. Carbon 117:421–26.

Zhu, Jianchao, Tao Zhang, Mansour Faried, and Wengang Chen. 2017. 3D Printing Cement

Based Ink, and It's Application within the Construction Industry. MATEC Web of Conferences 120:1–13.